Computer Modeling Study of the Effect of Hydration on the Stability of a Silica Nanotube

Nora H. de Leeuw,*,†,‡ Zhimei Du,†,‡ Ju Li,§ Sidney Yip,‖ and Ting Zhu‖

School of Crystallography, Birkbeck College, University of London, Malet Street, London WC1E 7HX, U.K., Department of Chemistry, University College London, 20 Gordon Street, London WC1H 0AJ, U.K., Department of Materials Science and Engineering, The Ohio State University, Columbus, Ohio 43210, and Department of Nuclear Engineering, Massachusetts Institute of Technology, Cambridge, Massachusetts 02139

ABSTRACT

Computer modeling techniques, which were employed to investigate the effect of water on the reactivity and stability of a SiO_2 nanotube, show that the side of the nanotube is relatively resistant to dissociative chemisorption and silicon dissolution but that the end of the nanotube is highly reactive toward water and amenable to dissolution. This finding is important for modern applications of nanostructures in fields ranging from catalysis to controlled drug release.

With the onset of the application of nanoscale materials to, for example, modern catalytic processes, research into structure/property relationships of promising materials such as carbon and oxide nanoparticles has increased dramatically (e.g., ref 1). This field is particularly suitable for investigation by modern computational techniques because experimental studies of many chemical phenomena at this scale are still difficult to perform. SiO_2 is a material with interesting properties on many different length scales, and given its importance in electronic, optical, and biomedical applications as well as its dominance in geological environments, it has particular appeal to a variety of scientific communities. In recent years, many unusual silica nanostructures have been synthesized by a variety of methods, from vapor deposition of silica thin films,[2] ribbons,[3] and wires[4] through the hydrothermal synthesis of quartz nanocrystals[5] to templated sol−gel techniques for the production of smart silica nanotubes for biomedical applications.[6]

The presence of water in the lattice affects physical properties such as diffusion rates and the melting point and is well known to reduce the crystal strength of bulk silicate materials (hydrolytic weakening),[7] allowing the deformation of the crystal. Although the interaction of water with both bulk and extended surface systems of silicate materials has

been investigated in a number of computational and experimental studies,[8−12] the present work is to the authors' knowledge the first study of the effect of hydration on the structure and stability of an SiO_2 nanoparticle. The model silica particle that we have chosen to study is a short nanotube consisting of 36 SiO_2 units, leading to structures of between 180 and 200 species for the anhydrous and hydrated tubes, respectively. In this work, we investigate the associative and dissociative adsorption of water at the sides and ends of the nanotube, with a view to determining whether the silica tube is a stable structure in the presence of water vapor and as such whether we could expect it to be synthesized in the future.

Computational methods are well placed to calculate at the atomic level the geometry and adsorption energies of water at the nanotube walls. The approach we have used is to employ classical energy-minimization techniques to study the energies of associative and dissociative adsorption of water at the different surface sites of the nanotube as well as the energies of dissolution of a silicon ion from the tube. The computer simulation code used for the calculation of the (hydrated) nanotube structures and energies was META-DISE,[13] which is designed to model bulk solid materials as well as dislocations, surfaces, and interfaces, where a Newton−Raphson procedure is used for the energy minimization. This code has been successful in modeling surface structures, energies, and adsorption processes of a range of (semi) ionic systems, including silicate materials such as α-quartz and microporous zeolite structures.[12,14,15] The

* Corresponding author. E-mail: n.deleeuw@mail.cryst.bbk.ac.uk. Fax: 020-7631 6803. Tel: 020-7679 7465.
† Birkbeck College London.
‡ University College London.
§ The Ohio State University.
‖ Massachusetts Institute of Technology.

simulations were executed using 3D periodic boundary conditions with the nanotube confined in a simulation cell of 10 nm × 10 nm × 10 nm, which ensured that interactions between the nanotube and its mirror images were negligible.

We have employed established Born-type potential models for the silicate framework and water molecules,[12,16,17] which have been shown to give accurate agreement with experimental hydration studies of quartz surfaces.[11] The interactions between the simulated species are described by long-range electrostatic forces and short-range forces, including the van der Waals interactions and short-range repulsions. The structure of the anhydrous nanotube was modeled by both the Sanders[16] and BKS[18] potential models to test the effect of different potential models on the optimized geometry, but because the resulting structures were very similar, the Sanders potential was used for the hydration calculations because this potential model is compatible with the polarizable potential model for water.

In addition, we compared our potential model with electronic structure calculations by simulating the adsorption of water at the (0001) surface of a slab of α-quartz material using established density functional theory (DFT) techniques within the generalized gradient approximation.[19,20] We modeled both a (0001) surface where all surface species were fully coordinated by O−Si−O bridges at the surface and a bulk-terminated (0001) surface with undercoordinated Si and O species.[12] At the fully coordinated surface, associative adsorption of the water molecules occurred, whereas dissociative adsorption and hence hydroxylation of the surface occurred when the surface contained dangling bonds. The adsorption energy for associative adsorption calculated by the DFT method was −45.3 kJ mol^{-1}, which is in good agreement with the interatomic potential calculation of −56.9 kJ mol^{-1}. Dissociative adsorption of water at the bulk-terminated surface was calculated to release 140.7 kJ mol^{-1} compared to 213.7 kJ mol^{-1} for the interatomic potential calculation. Despite the discrepancies between the two methods in the latter calculations, we consider the interatomic potential-based results to be adequate for our present purpose. We note that the potential model for hydroxy groups in silicate materials was carefully derived and tested using several quantum mechanical and experimental data points;[17] moreover, the calculated value of 213.7 kJ mol^{-1} for dissociative adsorption of water at the (0001) surface using the interatomic potential method agrees very well with experimental temperature-programmed desorption measurements by Fubini et al.,[21] who measured adsorption energies of approximately −200 kJ mol^{-1} for dissociative adsorption at the quartz surface. As such, we consider the potential model to be sufficiently reliable to be used in this study of the hydration of nanoparticulate silicate.

The nanotube is constructed of six hexagonal planar six-membered rings, each containing six silicon and six oxygen atoms (Figure 1a), and these interior rings are linked to each other by six bridging oxygen atoms, hence forming a network of corner-sharing SiO$_4$ tetrahedra. To retain the stoichiometry, the end rings are capped at both ends by three oxygens rather than six, leading to rings with alternating fully four-
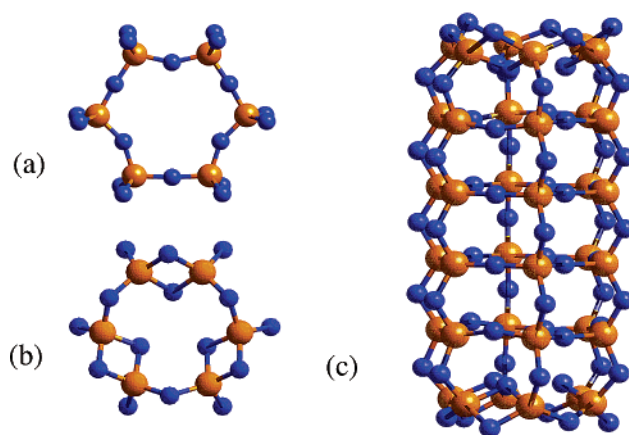

Figure 1. Geometry-optimized structure of the (a) interior layer, (b) end layer, and (c) complete SiO$_2$ nanotube (Si = orange, O = blue).

coordinated Si atoms and three-coordinated Si atoms. The three final oxygen atoms also have dangling bonds, being coordinated to only one silicon atom each. When the structure is geometry-optimized using the methods outlined above, these three oxygens spontaneously relax to form bridges to the three-coordinated Si atoms, leading to alternating single and double oxygen bridges between the silicon atoms, even though this entails the formation of strained edge-sharing SiO$_4$ tetrahedra (Figure 1b). The resulting structure is a stoichiometric silica nanotube with the bulk built of corner-linked SiO$_4$ tetrahedra, where all Si and O atoms are four- and two-coordinated, respectively (Figure 1c), but capped by three single and three double oxygen bridges at each end.

The size and geometry of the nanotube rings are similar to the channels in α-quartz or the six-rings in microporous silicate materials such as zeolites, and the outer wall of the tube resembles the α-quartz (0001) surface, where all Si and O atoms are fully coordinated without the presence of dangling bonds. Moreover, the hexagonal six-rings of the nanotube structure exist in natural cyclosilicate materials such as beryl, which contains columns formed of rings consisting of six SiO$_4$ tetrahedra linked by Be and Al ions, where interstitial species such as water molecules and foreign cations are found in the channels.[22] The lattice energy of the nanorod per SiO$_2$ unit is calculated to be within 30 kJ mol^{-1} of the average lattice energy per SiO$_2$ unit in a thin slab of α-quartz (∼3 nm) terminated by two (0001) surfaces, indicating that the silica nanotube structure is of comparable stability to thin silicate wafers. Thin slabs of silicate and other materials are routinely used in computational studies to model surface structures and processes,[23,24] and cluster models are often used to study reactive sites and defects in extended silicate systems.[9] Such calculations have been found to give reliable and accurate results, and we thus consider our silica nanotube structure to be a viable model for nanoparticulate silicate, which will give meaningful insights into the reaction of water with strained Si−O bonds in silica nanoparticles.

The hydration energy of the SiO$_2$ nanotube is given by eq 1:

$$E_{hydr} = E_{nano+wat} - (E_{nano} + E_{H_2O}) \qquad (1)$$

where E_{hydr} is the energy of adsorption of a water molecule at the nanotube, $E_{nano+wat}$ and E_{nano} are the calculated energies of the hydrated and dehydrated nanotubes, respectively, and E_{H_2O} is the self energy of water. For the associatively adsorbed water molecule, E_{H_2O} is straightforward and calculated to be -869.8 kJ mol^{-1}, but for the dissociated water molecule, the energy of dissociation is required as well, and E_{H_2O} here has a value of $+808.9$ kJ mol^{-1}. Full details are given in ref 12.

We first investigated the energies of adsorption of associated water molecules to a variety of sites on the SiO_2 nanotube. A large range of possible starting configurations was sampled to ensure that upon relaxation the true lowest-energy position rather than a local minimum was obtained. As such, initial configurations of the water molecules included adsorbing them by their oxygen atom to Si sites and by their hydrogens to oxygen atoms on the tube wall. We found, however, that even when the water molecule was initially positioned with its hydrogen atoms directed toward surface oxygen atoms and its oxygen atom pointing away from the tube side, the $Si-O_{water}$ interactions were sufficiently large so that in the final position the water molecule also coordinated through its oxygen atom to one or two surface silicons at about 2.76 Å at the wall of the tube (Figure 2a) and 2.30 Å at the end while hydrogen bonded to surface oxygen atoms at 1.85−2.16 Å. This type of associative physisorption of molecular water, without the formation of a $Si-O_{water}$ chemical bond, was also observed on the quartz (0001) surface, which similarly consists of fully coordinated SiO_2 units[12] and was confirmed by the electronic structure calculations of a slab of quartz material. In addition, this preference for interaction of the water molecule's oxygen atom with the cation rather than hydrogen bonding to surface oxygen atoms is also seen in ionic or other semicovalent systems, where both quantum mechanical calculations and atomistic simulations identified the cation−oxygen interaction as the major adsorption feature when water adsorbed in a molecular fashion.[25−27]

Although it is not possible to separate completely the $Si-O_{water}$ and $H-O_{tube}$ interactions for the adsorbed water molecules, we can quantify the $Si-O_{water}$ interaction to some extent by way of the hydration energies given in Table 1. For the potential model used for the water molecule in this study, the formation of a single hydrogen bond of 1.8 Å releases 20.2 kJ mol^{-1}, which agrees well with the experimental value of 22.1 kJ mol^{-1}.[28] At the end ring, where the $Si-O_{water}$ interaction is more significant, the adsorbed water molecule forms one hydrogen-bonded interaction to a surface oxygen atom at 1.85 Å, which should hence release approximately 20 kJ mol^{-1}. The energy released upon hydration is -63.4 kJ mol^{-1}, and the $Si-O_{water}$ interaction thus accounts for a maximum of approximately 43 kJ mol^{-1}, which is more than the energy of two $H-O_{tube}$ hydrogen bonds and is thus clearly the preferred interaction between the water molecule and the silica nanotube, especially because the water molecule can form additional hydrogen bonds to the nanotube
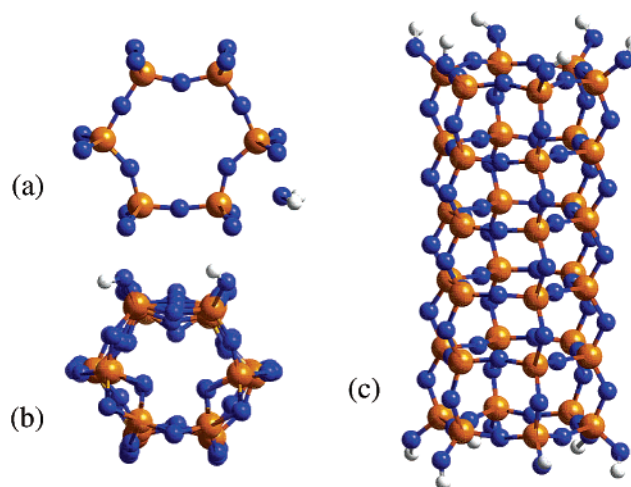

Figure 2. Geometry-optimized structure of the SiO_2 nanotube with (a) an associatively adsorbed water molecule at the side of the tube, (b) a dissociated water molecule at the end of the tube, and (c) three dissociated water molecules adsorbed at the two end rings, leading to a fully hydrogen-capped nanotube structure (Si = orange, O = blue, H = white).

Table 1. Hydration Energies of Associated and Dissociated Water at Different Surface Sites (kJ/mol)

position	associated	dissociated
end Si	−63.4	−511.3
wall Si	−45.5	−81.2

in addition to this $Si-O_{water}$ interaction. The hydration energies are similar for adsorption at silicon atoms on the side or at the end of the tube, although adsorption at the end of the tube is preferred by about 18 kJ mol^{-1}.

We next adsorbed dissociated water at the different sites, where the OH group was adsorbed to a surface silicon atom and the proton was adsorbed to a neighboring oxygen atom, which leads to the breaking of a $Si-O$ bond in the nanotube. Again, all possible starting configurations were investigated. From the hydration energies in Table 1, we see that dissociative adsorption of water at the nanotube wall is more favorable than associative adsorption at the same site by 35.7 kJ mol^{-1}. However, this difference in energy is sufficiently small that the driving force to dissociation of the associatively adsorbed water molecule will be small. In addition, substantial kinetic energy barriers to dissociative adsorption will also be expected. For example, breaking the $Si-O$ bond in the diatomic SiO molecule costs approximately 800 kJ mol^{-1}, and even though this process will probably be significantly less endothermic in an extended system such as the nanotube, where each silicon forms four $Si-O$ bonds, it will still be a formidable energy barrier to overcome. Associative adsorption would also agree with the same process in both bulk α-quartz, where electronic structure calculations have shown that interstitial water remains a molecular species,[26] and the quartz (0001) surface, which, like the nanotube, also contains fully coordinated Si and O atoms and where electronic structure calculations also show water to adsorb associatively, even to the extent that initially dissociated surface OH groups

recombine to form water molecules upon electronic and geometry optimization.

However, dissociative adsorption of water at an end silicon atom, leading to two vicinal hydroxy groups at the end of the nanotube (Figure 2b), releases a very large amount of hydration energy (511 kJ mol^{-1}), which is clearly in the realm of dissociative chemisorption and in excess of the adsorption energies found for even the most reactive of quartz surfaces (<465 kJ mol^{-1}).[12] The two vicinal hydroxy groups replace one of the two oxygen bridges between the two SiOH groups, leading to normal tetrahedral O$-$Si$-$O angles for these two silicon atoms and corner-sharing SiO$_4$ units. The resulting structure is thus less strained than the original anhydrous nanotube, leading to the release of this large amount of energy. Although the Si$-$O bond lengths in the relaxed nanotube at 1.59$-$1.70 Å resemble that of bulk quartz (1.61 Å), the Si$-$O$-$Si angles in the middle of the nanostructure at 152$-$176° are larger than in bulk quartz (141.3°), whereas in the single oxygen bridges of the end ring they are smaller by about 15°. However, it is the divergence of the O$-$Si$-$O and Si$-$O$-$Si angles in the double oxygen bridges within the end rings away from the equilibrium angles of bulk quartz to very small angles of as low as 83 and 95$-$118°, respectively, that causes the strain in the end-ring structure. Even though the double oxygen bridges formed spontaneously and are stable with respect to undercoordinated Si and O species at the end of the tube, dissociative adsorption of water at the end ring breaks one of these double Si$-$O$-$Si bridges, leading to normal tetrahedral O$-$Si$-$OH angles with the consequent release of very large amounts of hydration energy, suggesting that the oxygen atoms of the end ring would prefer to be capped by hydrogen atoms rather than O$-$Si$-$O bridges.

To test this hypothesis further, we calculated the formation of isolated hydroxy groups on both the end and the wall of the nanotube, which would also give an indication of the likelihood of surface diffusion of the hydroxy groups on the nanotube. On the wall, the formation of isolated hydroxy groups is an increasingly endothermic process costing from 104 to 186 kJ mol^{-1} for positions from two to six sites apart as low-coordinated surface species are created and hydrogen-bonded interactions between the two OH groups are lost as the distance between them increases. It is clear from these energies that we can expect no significant surface diffusion of any adsorbed hydroxy groups away from the vicinal positions. On the end sites, the formation of hydroxy groups two sites apart, which also led to the split of one double oxygen bridge, had little effect on the hydration energy (−501 kJ mol^{-1}), but when the hydroxy groups were fully isolated on either side of the end ring, the process was much less exothermic at −352 kJ mol^{-1}. In this case, the attachment of the hydroxy group to a silicon atom also leads to the fracture of one of the double oxygen bridges but with the formation of an undercoordinated ring oxygen and hence a dangling bond, which was no longer capped by a proton. This is a much less stable structure, hence leading to the smaller hydration energy.

Finally, we fully hydrated the two end rings by dissociated water molecules, three at each ring, to investigate whether the nanotube structure is preferentially terminated by complete oxygen rings (containing six instead of three oxygen atoms), which are all capped by hydrogen atoms to remove the dangling bonds of the terminating oxygen atoms rather than forming double oxygen bridges between the end silicon atoms. The calculated process is equal to adding three water molecules to each end ring according to eq 1. The average hydration energy released in this process is calculated to be −472.9 kJ mol^{-1} per water molecule, and it is thus clear that this hydrogen-capped structure will be the preferred state of the silica nanorod (Figure 2c).

Our results so far show that the end rings of the silica nanotube will be fully hydrated by dissociatively adsorbed water molecules, leading to an unstrained structure where the end oxygen rings are capped by hydrogen atoms. However, we are also interested to know whether the hydration of the end of the tube will progress beyond a fully protonated end ring and hence lead to the dissolution of the nanotube. We therefore investigated the sequential dissociative adsorption of four water molecules to one silicon atom at the end ring of the nanotube with the formation of two geminal hydroxy groups and the eventual dissolution of this Si atom and its replacement by four protons according to the process in eq 2:

$$Si_{Si} + 4H_2O_{(g)} = 4H_{Si} + Si(OH)_{4(g)} \tag{2}$$
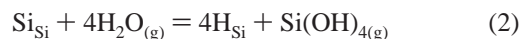
where Si$_{Si}$ is a silicon atom at a silicon site in the nanotube and H$_{Si}$ is a proton adsorbed at a silicon site. This process was calculated to be energetically favorable in bulk α-quartz and it is a well-known defect structure in many silicate materials.[26] For the sake of completeness, we have calculated this dissolution of an end Si atom for both the anhydrous and hydrogen-capped structure to evaluate whether the presence of the remaining double oxygen bridges in the anhydrous tube makes a difference to the dissolution energies.

Table 2 shows the energies released when consecutive dissociated water molecules are adsorbed to one silicon in an end ring, where the addition of each water molecule adds another OH group to the silicon and a proton to a neighboring oxygen. Eventually, the silicon atom is bonded to four OH groups and is detached from the nanotube, where the vacancy is surrounded by four OH groups. The two structures are shown in Figure 3, from which we see that the structure of the defect is similar for both tube structures. However, unlike the same defect in bulk quartz, the four protons are not all pointing toward the silicon vacancy, but two are angled away from the vacancy to retain the tetrahedral O$-$Si$-$OH angles. The silicon vacancy and the two protons pointing toward the vacancy site are indicated by arrows at the top of Figure 3. We see from Table 2 that the addition of the first three water molecules is exothermic for both structures, although the addition of the second dissociated water molecule to the anhydrous structure, breaking Si$-$O bond number 2 at the bottom of Figure 3a, releases about 3 times as much energy as the second water molecule added to the hydrogen-capped structure. Again, this effect is due to the strained structure
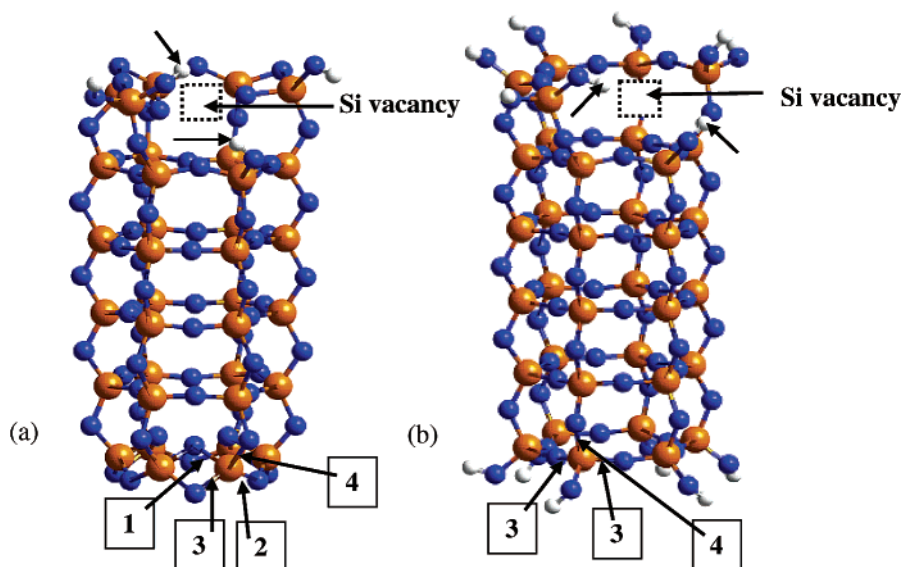
Figure 3. Geometry-optimized structures of (a) the anhydrous SiO_2 nanotube with one end silicon atom replaced by four protons and (b) the hydrogen-capped nanotube also with one Si dissolved from the structure. The protons pointing toward the Si vacancy are indicated by arrows at the top, whereas the relative strengths of Si−O bonds are numbered 1−4, from weak to strong, at the bottom (Si = orange, O = blue, H = white).

Table 2. Sequential Energies of Dissociative Hydration of the End Rings of the Nanotube for the Anhydrous and Fully Hydrogen-Capped Structures, Leading to the Dissolution of One Si Atom from One of the End Rings

	sequential hydration energies (kJ/mol)	
number of water molecules	anhydrous structure	hydrogen-capped structure
1	−511.3	
2	−133.0	−43.3
3	−42.7	−41.2
4	+11.6	+24.6

of the anhydrous tube, where after the breaking of one of the three double oxygen bonds by the first water molecule, labeled 1 in Figure 3a, the addition of a second water molecule breaks one of the single oxygen bridges labelled 2, hence opening up the end-ring structure and enabling the neighboring SiO_4 unit to rotate into a more favorable configuration, even though it is still attached by a double oxygen bridge to the next silicon. The addition of the third water molecule does not have much effect on the anhydrous structure, and the energies of the two nanotube structures are hence very similar. The broken Si−O bonds are the same for both structures and are labeled 3 in Figure 3a and b. The addition of the fourth water molecule with the formation of the $Si(OH)_4$ species, breaking the last Si−O bonds labeled 4 in Figure 3a and b, is less straightforward. If the $Si(OH)_4$ species remains closely associated with the nanostructure through hydrogen bonding, then the process is slightly endothermic (Table 2). However, if the $Si(OH)_4$ molecule is removed infinitely far from the now defective nanostructure, then the last step becomes much more endothermic—by 69 kJ mol^{-1} for the anhydrous structure and 51 kJ mol^{-1} for the hydrogen-capped structure—and the $Si(OH)_4$ molecule is thus unlikely to become completely detached from the nanotube. However, both anhydrous and hydrogen-capped nanotubes are clearly amenable to significant disruption and fragmentation of their structure by water, even though they are marginally resistant toward the complete dissolution of silicon atoms in the end rings.

In conclusion, our detailed calculations have shown that the side of a silica nanotube is relatively resistant to attack by water because the nondestructive associative physisorption of water is unlikely to be followed by the dissociative adsorption of water with consequent breaking of Si−O bonds, which is energetically not much more favorable. However, the atoms at the end of the nanotube are highly reactive toward water not only initially because of the strained environment of the end ring in the anhydrous tube but also because the structure is easily destroyed even further by the dissociative chemisorption of water and possibly by the replacement of silicons by protons. Even the hydrogen-capped nanotube structure is not immune to the hydrolysis of additional Si−O bonds, although the final Si−O bond, which links the silicon atom in the end ring to the oxygen atom bridging to the next six-ring, is thermodynamically just stable against dissolution by dissociative water. From our calculations, it is clear that long nanotubes or closed structures will be significantly more resistant against dissolution than short open-ended structures. Because the ends of this nanotube are only metastable in the presence of water, the synthesis of this structure will be a challenge for experimental solid-state chemists.

References

(1) Niederberger, M.; Barti, M. H.; Stucky, G. D. *J. Am. Chem. Soc.* **2002**, *124*, 13642.

(2) Nishiyama, N.; Tanaka, S.; Egashira, Y.; Oku, Y.; Ueyama, K. *Chem. Mater.* **2003**, *15*, 1006.

(3) Zach, M. P.; Newberg, J. T.; Sierra, L.; Hemminger, J. C.; Penner, R. M. *J. Phys. Chem. B* **2003**, *107*, 5393.

(4) Zhang, H.-F.; Wang, C.-M.; Buck, E. C.; Wang, L.-S. *Nano Lett.* **2003**, *3*, 577.

(5) Bertone, J. F.; Cizeron, J.; Wahi, R. K.; Bosworth, J. K.; Colvin, V. L. *Nano Lett.* **2003**, *3*, 655.

(6) Mitchell, D. T.; Lee, S. B.; Trofin, L.; Li, N.; Nevanen, T. K.; Söderlund, H.; Martin, C. R. *J. Am. Chem. Soc.* **2002**, *124*, 11864.

(7) Griggs, D. T.; Blacic, J. D. *Science* **1965**, *147*, 292.

(8) Reuschle, T.; Darot, M. *Eur. J. Mineral.* **1996**, *8*, 695.

(9) Purton, J.; Jones, R.; Heggie, M.; Oberg, S.; Catlow, C. R. A. *Phys. Chem. Miner.* **1992**, *18*, 389.

(10) Jones, R.; Oberg, S.; Heggie, M. I.; Tole, P. *Philos. Mag. Lett.* **1992**, *66*, 61.

(11) Sneh, O.; George, S. M. *J. Phys. Chem.* **1995**, *99*, 4639.

(12) de Leeuw, N. H.; Higgins, F. M.; Parker, S. C. *J. Phys. Chem. B* **1999**, *103*, 1270.

(13) Watson, G. W.; Kelsey, E. T.; de Leeuw, N. H.; Harris, D. J.; Parker, S. C. *J. Chem. Soc., Faraday Trans.* **1996**, *92*, 433.

(14) Slater, B.; Titiloye, J. O.; Higgins, F. M.; Parker, S. C. *Curr. Opin. Solid State Mater. Sci.* **2001**, *5*, 417.

(15) Higgins, F. M.; de Leeuw, N. H.; Parker, S. C. *J. Mater. Chem.* **2002**, *12*, 124.

(16) Sanders, M. J.; Leslie, M.; Catlow, C. R. A. *J. Chem. Soc., Chem. Commun.* **1984**, 1271.

(17) Baram, P. S.; Parker, S. C. *Philos. Mag. B* **1996**, *73*, 49.

(18) van Beest, B. W. H.; Kramer, G. J.; van Santen, R. A. *Phys. Rev. Lett.* **1990**, *64*, 1955.

(19) Kresse, G.; Hafner, J. *Phys. Rev. B* **1993**, *47*, 5858. Kresse, G.; Hafner, J. *Phys. Rev. B* **1994**, *49*, 14251.

(20) Kresse, G.; Furthmüller, J. *J. Comput. Mater. Sci.* **1996**, *6*, 15. Kresse, G.; Furthmüller, J. *Phys. Rev. B* **1996**, *54*, 11169.

(21) Fubini, B.; Bolis, V.; Bailes, M.; Stone, F. *Solid State Ionics* **1989**, *32*, 258.

(22) Deer, W. A.; Howie, R. A.; Zussman, J. *An Introduction to the Rock-Forming Minerals*, 2nd ed.; Longman Scientific & Technical: Essex, England, 1992.

(23) Rignanese, G.-M.; De Vita, A.; Charlier, J.-C.; Gonze, X.; Car, R. *Phys. Rev. E* **2000**, *61*, 13250.

(24) Greathouse, J. A.; O'Brien, R. J.; Bemis, G.; Pabalan, R. T. *J. Phys. Chem. B* **2002**, *106*, 1646.

(25) de Leeuw, N. H.; Purton, J. A. *Phys. Rev. B* **2001**, *63*, 5417.

(26) de Leeuw, N. H. *J. Phys. Chem. B* **2001**, *105*, 9747.

(27) Cooper, T. G.; de Leeuw, N. H. *Surf. Sci.* **2003**, *531*, 159.

(28) Curtiss, L. A.; Frurip, D. J.; Blander, M. *J. Chem. Phys.* **1979**, *71*, 2703.